Article

Applied Spectroscopy
2018, Vol. 72(12) 1764–1773

DOI: 10.1177/0003702818798405
journals.sagepub.com/home/asp
SAGE

Quantifying Graphene Oxide Reduction Using Spectroscopic Techniques: A Chemometric Analysis

Tejaswini Rama Bangalore Ramakrishna[1,2], Daniel Patrick Killeen[2], Tim David Nalder[1,2], Susan Nellette Marshall[2], Wenrong Yang[1], and Colin James Barrow[1]

Abstract

The surface chemistry of graphene oxide (GO) can be modified by the chemical reduction of oxygen-containing groups using L-ascorbic acid (L-AA). Being able to "tune" the surface hydrophobicity of GO in a controlled manner, with a well-defined level of reduction, provides a valuable tool for understanding and controlling interactions with hydrophobic surfaces. Numerous analytical and chemical methods have been used to determine the extent of reduction in chemically reduced graphene oxide (CRGO) samples. However, many of these methods are limited by their laborious nature, cost, or lack of sensitivity in resolving oxygen content in samples that have only been reduced for short periods of time, making them inappropriate for rapid use with multiple samples. Here, we have used ultraviolet (UV), Raman, and attenuated total reflection infrared (ATR-IR) spectroscopy to monitor the chemical reduction of GO. These three techniques are simple, rapid, nondestructive, accurate, and widely available. The data set from each technique has been correlated and modeled against a reference data set (carbon to oxygen ratio obtained from elemental analysis) using partial least squares regression (PSLR). Using this approach, the chemical reduction of GO was quantified from UV ($r^2 = 0.983$, $RMSE_{CV} = 0.049$), Raman ($r^2 = 0.961$, $RMSE_{CV} = 0.073$) and ATR-IR ($r^2 = 0.993$, $RMSE_{CV} = 0.032$) data. ATR-IR enabled identification of the different oxygen-containing groups on GO, and coupled with chemometric modeling, provides an excellent approach for the routine quantitative analysis of the chemical reduction of GO.

Keywords

Chemically reduced graphene oxides, CRGO, chemometric, graphene oxide, GO, partial least squares regression, PLSR, surface hydrophobicity

Date received: 5 April 2018; accepted: 13 August 2018

Introduction

Graphene can be produced from graphene oxide (GO) using many different reducing agents.[1–3] One of the cheapest, safest, and most readily available reagents for this purpose is L-ascorbic acid (L-AA), a mild reducing agent that reacts with oxygen moieties on the surface of GO sheets.[3] The reaction proceeds slowly, converting surface oxygen moieties on GO sheets to water, while L-AA is deprotonated to dehydroascorbic acid.[3] At the same time, oxalic and glucuronic acids, which form spontaneously from dehydroascorbic acid, react with the peripheral oxygen groups, e.g., carboxylic acids, which effectively caps them and interrupts π–π interactions between GO sheets.[3] This is accompanied by a decrease in sp^3 character and an increase in sp^2 "graphene-like" character on the sheets, which increases electronic conductivity and surface hydrophobicity.[3] These chemically reduced graphene oxides (CRGOs) are widely used in the fabrication of energy storage cells,[4,5] chemical sensors,[6,7] self-assembled monolayer-based electrodes,[8] and field effect transistors.[9,10]

[1]School of Life and Environmental Sciences, Deakin University, Geelong, VIC, Australia
[2]Seafood Unit, The New Zealand Institute for Plant & Food Research Limited, Nelson, New Zealand

Corresponding author:
Tim David Nalder, School of Life and Environmental Sciences, Deakin University, 75 Pigdons Road, Waurn Ponds 3216, VIC, Australia.
Email: tim.nalder@deakin.edu.au

The mild reducing conditions associated with L-AA solutions make it possible to produce chemically diverse CRGOs by varying the duration of the reaction.[3,11–13] Longer reduction times decrease the concentration of surface hydroxyl (OH), carbonyl (C=O), epoxy (C–O–C), and carboxyl (COOH) groups, which modulates the surface hydrophobicity of the CRGOs. This is sometimes known as "tuning" the surface hydrophobicity and can be used to produce CRGOs with diverse surface chemistries.[3,14,15] In addition to the applications listed above, these materials are useful in the field of enzyme immobilization, as the activity of various enzymes is highly dependent on the hydrophobicity of the solid phase to which they are bound.[12,13,16,17] Controlling the extent of chemical reduction is not straightforward and the analytical methods commonly used for determining the extent that CRGOs are reduced can be slow and expensive. Therefore, there is a need to develop rapid, quantitative analysis methods for determining the extent of reduction in CRGO samples.

Many analytical methods have been used to characterize CRGOs, including: elemental analysis,[18–20] X-ray photoelectron spectroscopy (XPS),[21–23] contact angle measurement,[24–26] X-ray diffraction (XRD),[27–29] thermal gravimetric analysis,[30–32] atomic force microscopy,[33–35] and nuclear magnetic resonance.[36–38] Chemical methods for characterizing CRGOs have also been employed, e.g., the use of $(Ru(bpy)_3)^{2+}$ and pyrene to determine the oxygen content.[14,15] In this work, we wanted to assess methods that could be performed using widely available instrumentation and that are also relatively rapid and nondestructive. While most of the methods mentioned above are able to structurally define the surface properties of GO/CRGOs, there are several shortcomings. First, many of these methods require instrumentation that is not widely available. Second, some of these methods, while suitable for showing clear differences between large steps in GO reduction (i.e., GO to a fully reduced CRGO), lack the sensitivity required to accurately determine small changes in reduction. For research fields, such as enzyme immobilization that greatly relies upon being able to monitor minor changes to surface hydrophobicity, precisely measuring these properties is important. Thus, methods investigated needed to be suitably sensitive for determining small changes in reduction.

Herein we have assessed ultraviolet (UV), attenuated total reflection infrared (ATR-IR), and Raman spectroscopies.

Several reports have demonstrated the potential of these methods for characterizing CRGOs,[35,39–43] but to our knowledge, data from these techniques has not been modeled against reference data to produce quantitative chemometric models. Elemental analysis was used as the reference method to accurately quantitate the mass proportion of C, H, N, and O in CRGOs that had been reduced over a range of time points.[43] Results from the analysis were used to model structured variance in UV, Raman, and IR spectra of subsamples of the same CRGO sample set using partial least squares regression (PLSR).

Materials and Methods

Chemicals

Graphite flakes ($< 45\,\mu m$) and L-AA were purchased from Sigma Aldrich. Concentrated sulfuric acid and hydrochloric acid were purchased from Merck Millipore. Hydrogen peroxide (30% v/v) and potassium permanganate were purchased from Chem-Supply (Australia).

Preparation of Graphene Oxide

Graphene oxide was synthesized in solution using a modified Hummer's method.[44] Graphite flakes (2 g, Sigma-Aldrich) were dispersed in sulfuric acid (12 mL) and heated at 80 °C for 4.5 h. The mixture was cooled and graphite flakes were exfoliated for 5 h using an ultrasonicating bath (GRANXUBA3, VWR Industries). This solution was diluted with MilliQ H_2O (500 mL) and left to settle for 12 h. The pre-oxidized graphite flakes were filtered through an Isopore membrane filter (0.2 μm pore size, 25 mm width) and dried in a hot air oven at 70 °C. The dried flakes were dispersed in sulfuric acid (120 mL), forming thin graphite oxide sheets. Potassium permanganate (15 g) was slowly added and the solution was stirred for 2 h at room temperature. This mixture was diluted with MilliQ H_2O (250 mL), stirred for 2 h, and then diluted with a further aliquot of MilliQ H_2O (700 mL). Hydrogen peroxide (30%, 20 mL) was added and the mixture was allowed to settle for 12 h. The resulting graphene oxide was divided into batches (15 mL) and centrifuged at 12 000 rpm (Eppendorf 5810 R, F-34-6-38 rotor) for 15 min. Pellets were resuspended in hydrochloric acid (10 mL, 10% v/v) to wash and remove any metal ions, followed by centrifugation at 12 000 rpm for 15 min. Finally, pellets were washed with MilliQ H_2O and centrifuged repeatedly until thin GO sheets floated in the supernatant. The GO sheets were collected as an aqueous dispersion in MilliQ H_2O. Aliquots (1 mL) were then dried at 60 °C in an oven to quantify the weight of GO in solution. After quantification the concentration of GO was adjusted to ~ 2 mg mL^{-1} by addition of MilliQ H_2O.

Chemical Reduction of Graphene Oxide

To synthesize CRGOs the aqueous dispersion of GO was chemically reduced using the L-AA method.[3] Three individual preparations of GO were used, with reduction initiated by adding L-AA (200 mg) into 20 mL GO solutions (2 mg mL^{-1}) in a 50 mL Schott bottle. The solutions were stirred (300 rpm) at room temperature (~22 °C), with the

reduction allowed to proceed for different lengths of time (2, 4, 6, 8, 12, 24, and 48 h). After the respective times CRGO samples were pelleted by centrifugation at 12 000 rpm (Eppendorf 5810 R, F-34-6-38 rotor) for 10 min and washed repeatedly with MilliQ H_2O to remove excess L-AA. Lastly, the synthesized CRGO pellets were resuspended in MilliQ H_2O to a concentration of 2 mg mL^{-1} and used in characterization studies including elemental analysis, UV, Raman, and ATR-IR spectrophotometric measurements.

Elemental Analysis

Elemental analyses were carried out by Campbell Microanalytical Laboratory (Department of Chemistry, University of Otago, New Zealand). Before analysis, samples were made to a concentration of 2 mg mL^{-1} in MilliQ water, freeze dried, and desiccated to remove residual moisture. The carbon (C), hydrogen (H), and nitrogen (N) contents were determined. The percentage of oxygen (O) was determined theoretically by mass balance, i.e., %O = 100 − [% C + % H + % N].

Ultraviolet Visible Spectroscopy

Absorbance spectra were measured from 200–700 nm using a Varian Cary 300 spectrometer (Agilent Technologies) using a scan rate of 500 nm min^{-1}. Solutions of GO and CRGOs in MilliQ water were presented in a quartz cuvette at a concentration of 67 μg mL^{-1}.

Raman Spectroscopy

Raman spectra of freeze dried GO and CRGO samples were acquired using a Reinshaw InVia microspectrometer (Reinshaw) equipped with a 50 × objective lens and charge-coupled device (CCD) detector. Spectra were acquired using a 180° backscattering geometry. Incident radiation was supplied by an argon ion laser, emitting at 514 nm, with a power of 2.5–5.0 mW, and a laser spot size of 1.5 μm. Each spectrum was calculated as the average of 5 × 2 s acquisitions, which recorded Stokes scattered light intensity at 940–2000 cm^{-1} with a spectral resolution of 4 cm^{-1}. Five spectra were acquired from different locations for each sample and averaged to produce the final spectrum. The laser was manually focused on the sample surface before each acquisition.

Attenuated Total Reflection Infrared Analysis

Infrared spectra were acquired at 4000–600 cm^{-1} using a Bruker Alpha ATR-IR spectrometer (Brucker Optik) equipped with a single reflection diamond crystal and a deuterated triglycine detector. Each spectrum was the average of 512 scans with a spectral resolution of 4 cm^{-1}. GO and CRGO samples (2 mg mL^{-1} solutions in MilliQ water) were drop cast directly onto the ATR crystal and allowed to dry into thin films before spectral acquisition.

Chemometric Analysis

Chemometric processing and analysis of the data sets was performed using The Unscrambler X software, version 10.3 (CAMO Software). Ultraviolet spectra were reduced to the region of 200–400 nm and their intensity was normalized using a standard normal variate (SNV) transformation. Raman spectra were subjected to a Savitzky–Golay second-order derivative transformation (second-order polynomial, 30-point symmetric kernel) and the spectral range of 1730–1180 cm^{-1} was then normalized using a SNV transformation. Infrared spectra were subjected to a Savitzky–Golay, second-order derivative transformation (second-order polynomial order, four-point symmetric kernel) and the spectral ranges of 3050–2700 cm^{-1} and 1900–800 cm^{-1} were normalized using a SNV transformation. Pre-processed spectra from these three spectroscopic methods were related to the C:O ratio of the CRGO sample sets using PLSR and the non-iterative partial least squares (NIPALS) algorithm. Models were validated using full, leave-one-out cross-validation.

Results and Discussion

Elemental Analysis of Chemically Reduced Graphene Oxides

The mass percentages of C, H, and N of the CRGO sample set were determined by elemental analysis (Table I). These results were used to calculate the mass % of O for each sample (Table I), which decreased in a linear fashion with increased reduction times ($r^2 = 0.980$, up to 24 h) (Fig. 1a). After 48 h the relationship deviated from linearity (Fig. 1b), indicating that the rate of reduction had changed. The reason for the nonlinear region beyond 24 h is most likely related to the reduced availability of surface oxygen groups as the reaction proceeds. During the reduction of GO, the physical state of the material gradually changes from being more hydrophilic to hydrophobic. Up to 24 h, the GO sheets remain dispersed, with the reduction of the surface oxygen groups able to proceed at a linear rate. However, after 24 h, CRGOs begin to aggregate, indicating that the reduction is nearing completion, with most of the oxygen functional groups removed from the surface, except the carboxylic groups at the edges. Previously, it has been suggested that solution-based processing methods are not efficient for the removal of carboxylic groups at the edges, with the groups remaining in extensively reduced CRGO samples.[41] Therefore, under the conditions used in this work it would appear that the 24 h time point represents an important threshold for obtaining stable CRGO

dispersions. Reduction of GO beyond 24 h results in aggregation, limiting the rate of L-AA-mediated reduction and resulting in a deviation from the linear relationship observed for less reduced CRGOs.

Table 1. Elemental composition (C, H, N, and O percent mass) of graphene oxide and chemically reduced graphene oxides, reduced for 2–48 h.

Sample	% C	% H	% N	% O	C : O ratio
Graphene oxide A	45.59	2.60	2.01	51.82	0.88
Graphene oxide B	45.16	2.36	1.49	52.48	0.86
2 h CRGO A	48.17	2.23	<0.3	49.61	0.97
2 h CRGO B	48.27	2.66	<0.3	49.08	0.98
2 h CRGO C	48.71	2.66	<0.3	48.64	1.00
4 h CRGO A	50.33	2.70	1.56	46.98	1.07
4 h CRGO B	50.32	2.40	1.51	47.28	1.06
4 h CRGO C	49.86	2.32	1.49	47.83	1.04
6 h CRGO A	50.98	2.52	1.14	46.51	1.10
6 h CRGO B	51.47	1.91	1.13	46.62	1.10
6 h CRGO C	51.56	1.91	1.13	46.53	1.11
8 h CRGO A	53.46	2.18	0.97	44.37	1.20
8 h CRGO B	53.80	1.94	0.94	44.26	1.22
8 h CRGO C	54.91	2.45	1.03	42.64	1.29
12 h CRGO A	57.03	2.34	0.97	40.64	1.40
12 h CRGO B	57.45	1.91	0.90	40.65	1.41
12 h CRGO C	58.14	1.87	0.82	40.00	1.45
24 h CRGO A	66.09	1.87	<0.3	32.05	2.06
24 h CRGO B	65.78	1.70	<0.3	32.53	2.02
24 h CRGO C	65.24	1.93	<0.3	32.84	1.99
48 h CRGO A	69.96	1.48	<0.3	28.56	2.45
48 h CRGO B	75.33	1.36	<0.3	23.32	3.23
48 h CRGO C	76.52	1.46	<0.3	22.04	3.47

A small amount of N, which diminished with increasing reduction times, was also detected in the samples (Table 1). The exact origin of N is unclear; one possible source is residual potassium permanganate ($KMNO_4$) that was used for synthesizing GO.

While elemental data could be used to accurately characterize the extent of reduction in the CRGO sample set, it required specialized analytical facilities and results in sample destruction. We wanted to assess whether UV and IR spectroscopies could be used for this analysis as they use widely available instrumentation and allow nondestructive analysis. We also assessed Raman spectroscopy, which allows straightforward sample presentation and rapid, nondestructive analysis. To assess the merits of these methods, we used PLSR to model structured variance in UV, IR, and Raman spectra against variance in C : O ratios calculated from elemental analysis data.

Ultraviolet–Visible Spectroscopy for Determining Extent of Reduction in Chemically Reduced Graphene Oxides

The UV spectra of the CRGO samples are presented in Fig. 2 and are consistent with UV data from similar sample sets, reported elsewhere.[45] The UV spectrum of GO had a peak maximum at 230 nm and a visible "shoulder peak" at 300 nm from π–π^* and n–π^* transitions, respectively. As reduction time increased, the UV maximum for the CRGOs gradually red shifted to 266 nm and the shoulder at 300 nm became less visible (Fig. 2). This was attributed to reduced energy of π–π^* transitions associated with increased conjugation on the CRGO sheets. These dynamic changes in UV absorbance wavelengths and intensities confounded linear regression models relating single wavelength intensities to C : O ratio reference values. We therefore related these reference values to the full (200–400 nm)

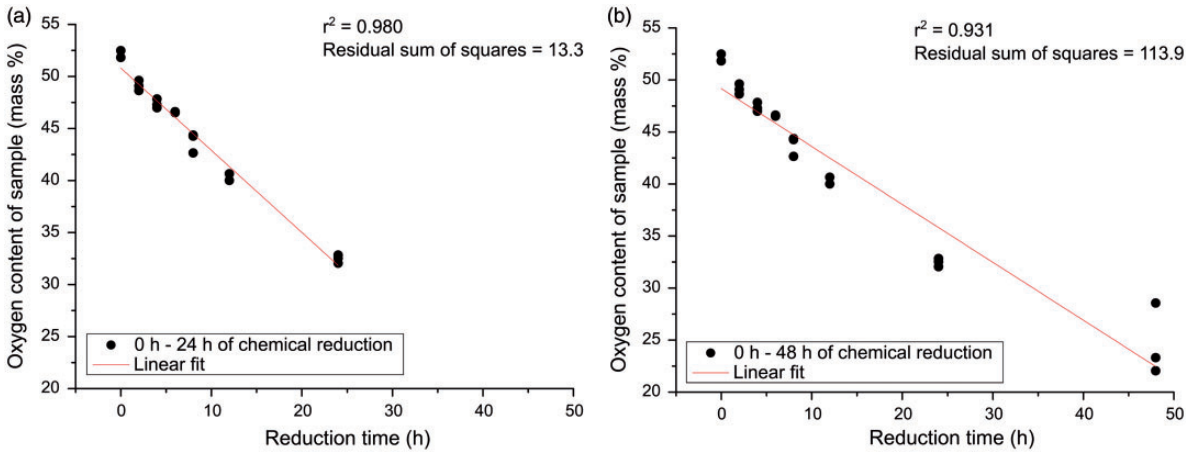

Figure 1. Linear regression of reduction time versus oxygen content of chemically reduced graphene oxide samples from (a) 0–24 h and (b) 0–48 h.

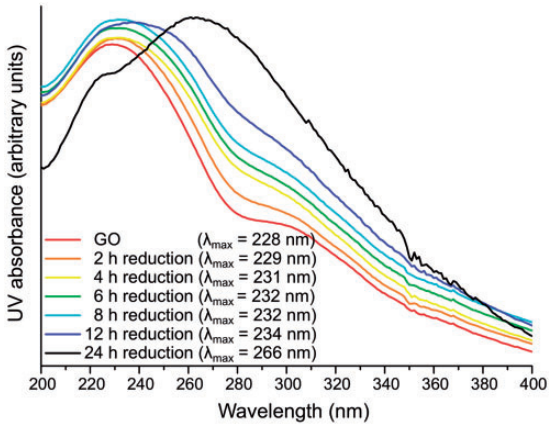

Figure 2. Ultraviolet spectra of graphene oxide and graphene oxides that have been chemically reduced by exposure to a solution of 10 mg mL^{-1} L-ascorbic acid for 2–24 h.

intensity-normalized UV spectra of the CRGO sample set using PLSR.

A summary of the PLSR model relating UV spectral variance to C : O ratios is presented in Fig. 3. The 48 h point was omitted as it did not fit the model, possibly due to the change in the reaction rate for this sample, as discussed above (Fig. 1). Due to the aggregated state, it is also possible that the dispersion of the 48 h sample in aqueous solution is affected, limiting its characterization by UV. Calibration and validation plots of the PLSR model are shown in Fig. 3a, demonstrating a good fit between UV spectral data and C : O ratios (validation $r^2 = 0.983$; root mean square error of cross-validation [$RMSE_{CV}$] = 0.049). The loadings plot in Fig. 3b shows that the model is largely derived from the variance in the spectral intensity at 230 and 277 nm, which are loaded inversely to one another. These inverse loadings imply that absorbance intensity at 230 nm deceases as chemical reduction proceeds, while the absorbance intensity at 277 nm increases. This pattern is consistent with an increase in π-conjugation with increasing reduction times applied to the CRGO samples.

Following inspection of the loadings plot, we assessed the ratio of UV absorbance. It was apparent that there was a latent relationship between the band intensities at 230 nm and 270 nm, and the extent of reduction in the CRGO samples. Therefore, we attempted to correlate the intensity ratio of these wavelengths with the C : O reference data determined by elemental analysis. However, these data were not well correlated, emphasizing the usefulness of simultaneously relating all UV spectral intensities to the reference data using PLSR. These results demonstrate that PLSR of UV spectra can be used to rapidly and accurately characterize the extent of oxidation that has occurred in CRGO samples. While this analytical technique was feasible, the method required samples to be analyzed in solution, which was not ideal. A more practical and rapid approach would enable analysis to be performed directly on dry samples. For this reason, we also investigated IR and Raman spectroscopy for this application.

Raman Spectroscopy for Determining Extent of Reduction in Chemically Reduced Graphene Oxides

Raman spectra of the CRGO sample set are presented in Fig. 4a and show two major spectral features, which have been described elsewhere as the "graphitic" G-band (1600 cm^{-1}) and the "defects" D-band (1330 cm^{-1}). The G-band derives intensity from C=C double bond stretching vibrations and the D-band derives intensity from bending vibrational modes associated with C–O bending modes.[3,23,46] The relative intensity of these bands have previously been used to determine the "end-point" of chemical reduction of graphene oxide.[3,23,46] Here, we go a step further, using the Raman intensity of these bands to quantitatively measure the extent of reduction in CRGO by relating Raman spectra to C : O ratios calculated from elemental analysis using PLSR. Before modeling, Raman spectra were subjected to pre-processing. The broad spectral features, including intensity offset (Fig. 4a), were removed by subjecting each spectrum to a second derivative transformation (Fig. 4b). Next, the spectral range was reduced to 1730–1180 cm^{-1}, which contained the G- and D-bands. Finally, a standard normal variate transformation was performed to normalize absolute spectral intensity (Fig. 4d).

A summary of the PLSR model relating Raman spectral variance to C : O ratios of the CRGO sample set is presented in Fig. 5. For the same reasons discussed above, i.e., poor fit, the 48 h time point was omitted from the model. The calibration and validation plots of the PLSR model are shown in Fig. 5a, demonstrating a good fit between Raman spectral variance and C : O ratios (validation $r^2 = 0.961$; $RMSE_{CV} = 0.073$). The loadings plot (Fig. 5b) demonstrated that the model was largely derived from spectral variance related to the G-band at 1600 cm^{-1}. The increased G-band intensity indicated an increase in the amount of double bonds, relative to C–O groups, which is consistent with an increase in π-character as CRGO samples are reduced to more closely resemble graphene. The PLSR model based on Raman spectral variance performed slightly worse that the UV spectroscopy-derived model, but had the added advantage of more straightforward sample presentation.

Attenuated Total Reflection Infrared Spectroscopy for Determining Extent of Reduction in Chemically Reduced Graphene Oxides

Spectral acquisition using ATR permitted rapid, nondestructive analyses of solid CRGO samples. Before modeling, spectra were subjected to pre-processing. Broad spectral features that did not contain molecular vibrational information (Fig. 6a) were removed by performing a second derivative transformation of each spectrum (Fig. 6b). The spectral

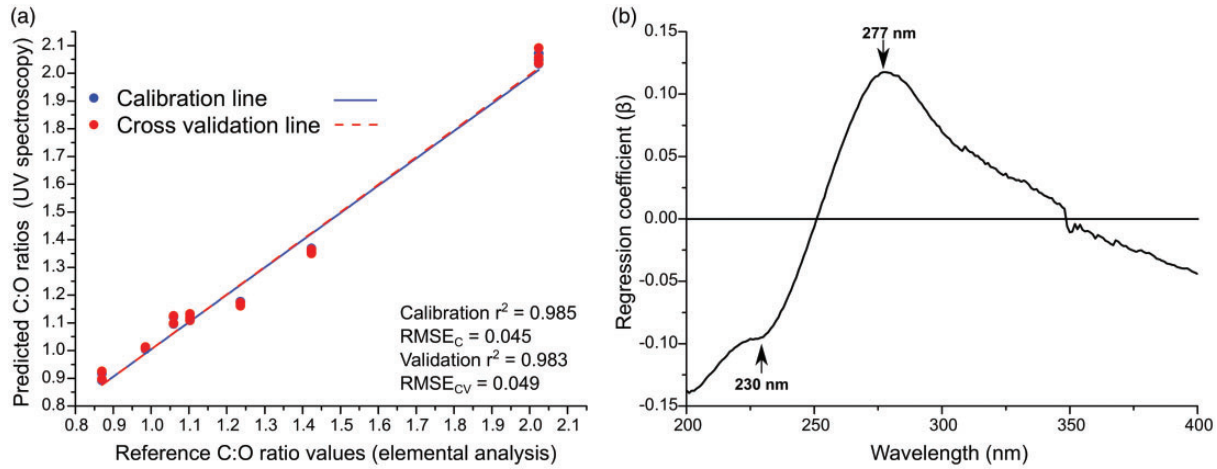

Figure 3. Summary of PLSR model relating C : O ratios of chemically reduced graphene oxide samples to UV spectral variance in the range of 200–400 nm. The (a) regression plots and (b) regression coefficient are shown.

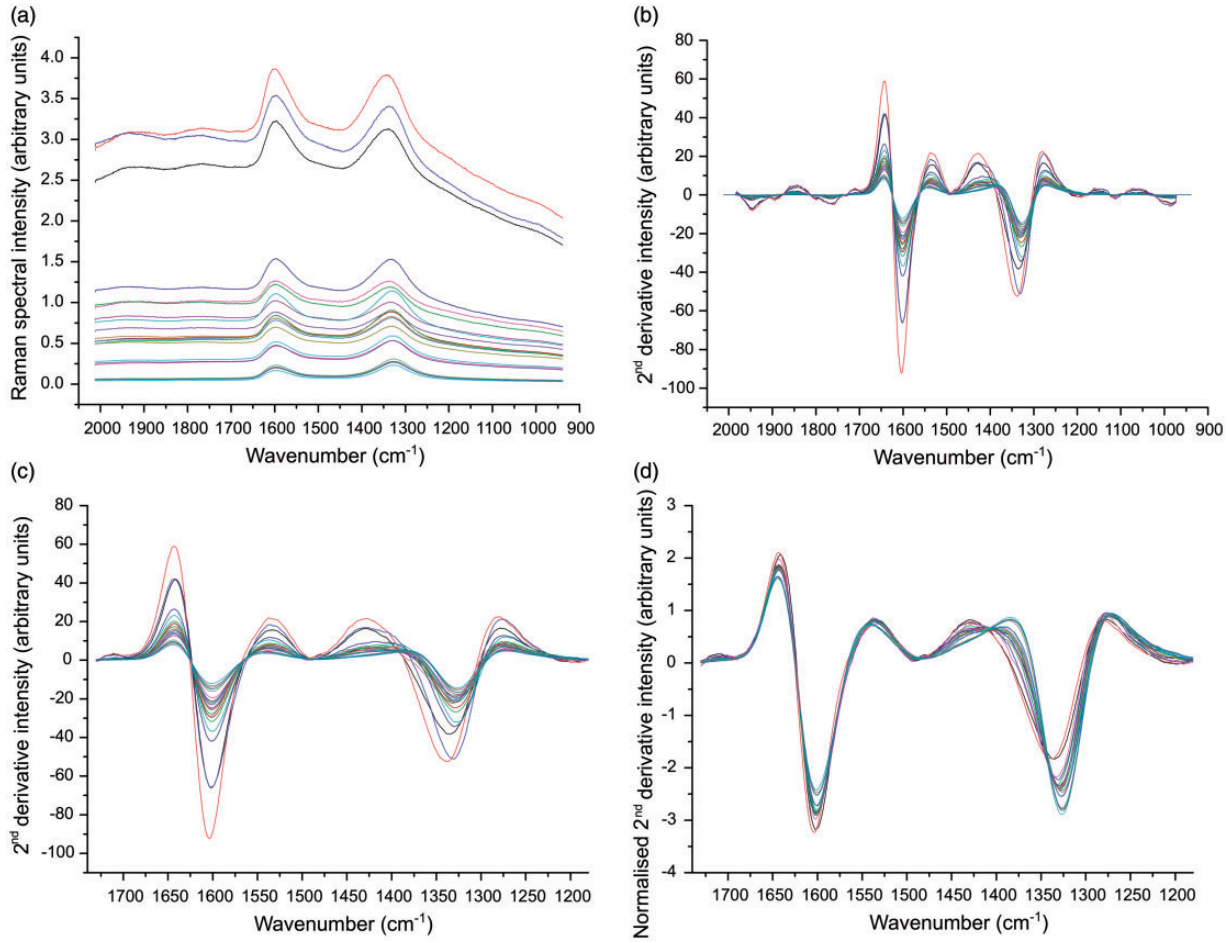

Figure 4. Summary of spectral pre-processing of Raman spectra of chemically reduced graphene oxide samples showing (a) raw spectral data, (b) spectra following second derivative transformation, (c) spectra following data reduction, and (d) spectra following standard normal variate transformation.

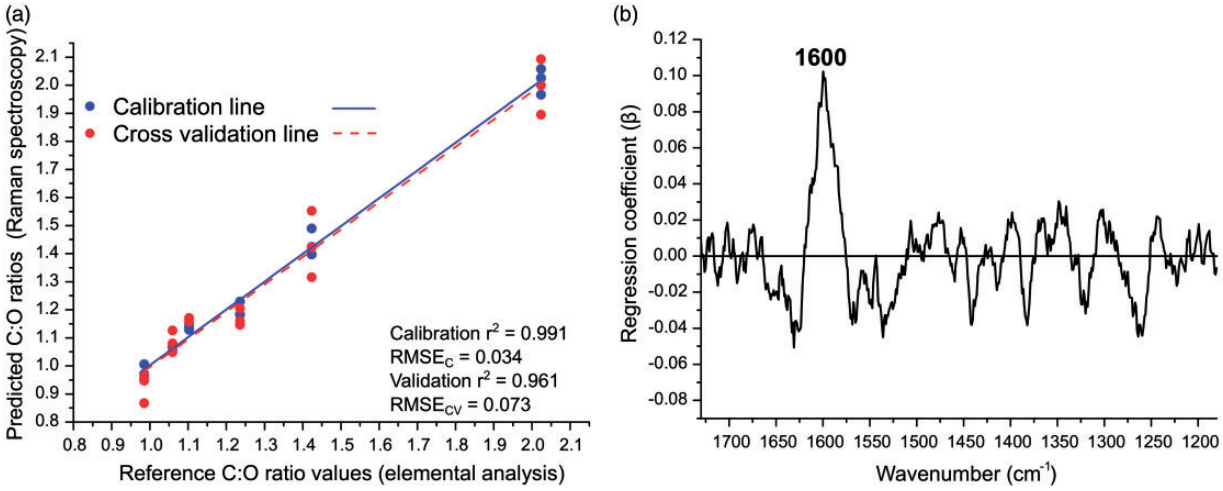

Figure 5. Summary of PLSR model relating C : O ratios of chemically reduced graphene oxide samples to Raman spectral variance in the range of 1750–1150 cm^{-1}. The (a) regression plots and (b) regression coefficient are shown.

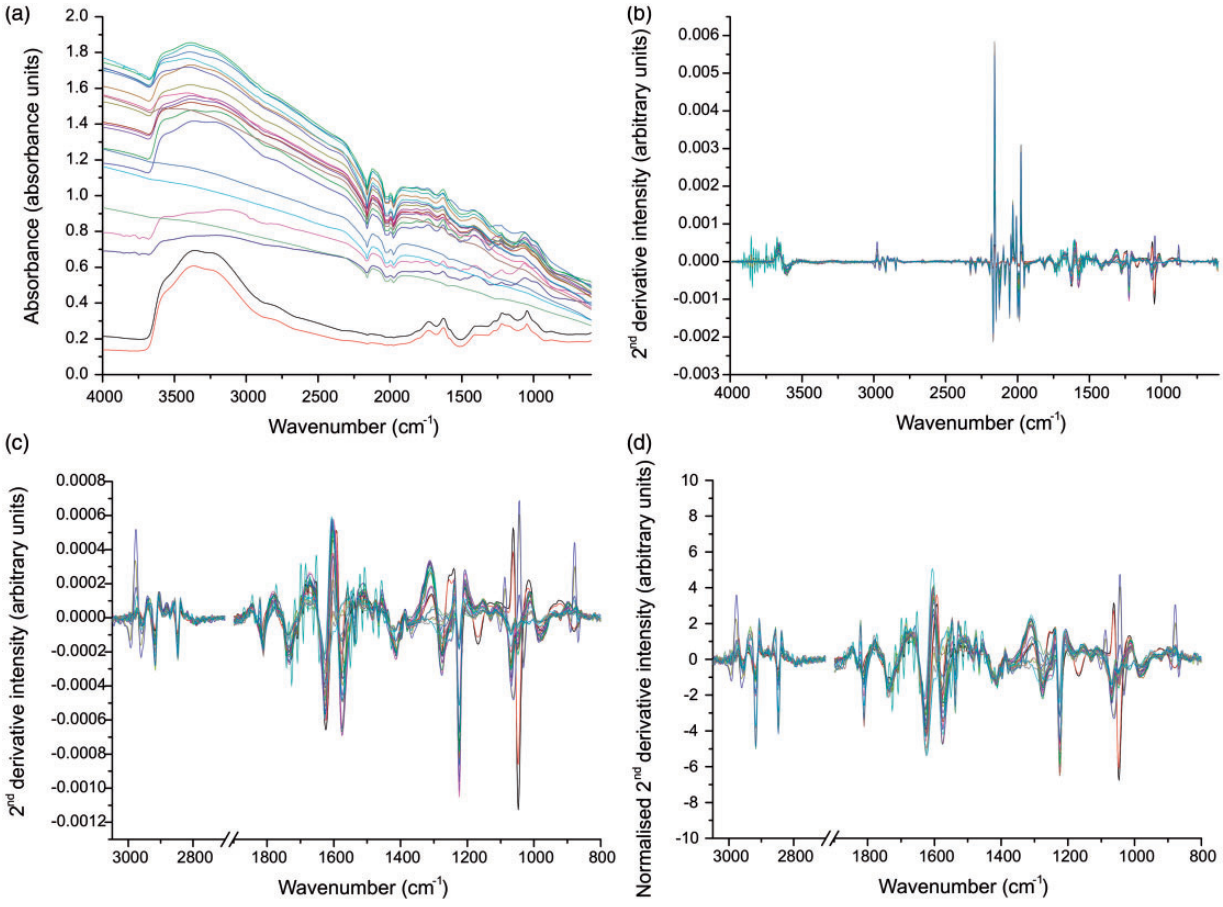

Figure 6. Summary of spectral pre-processing of IR spectra of chemically reduced graphene oxide samples showing (a) raw spectral data, (b) spectra following second derivative transformation, (c) spectra following data reduction, and (d) spectra following standard normal variate transformation.

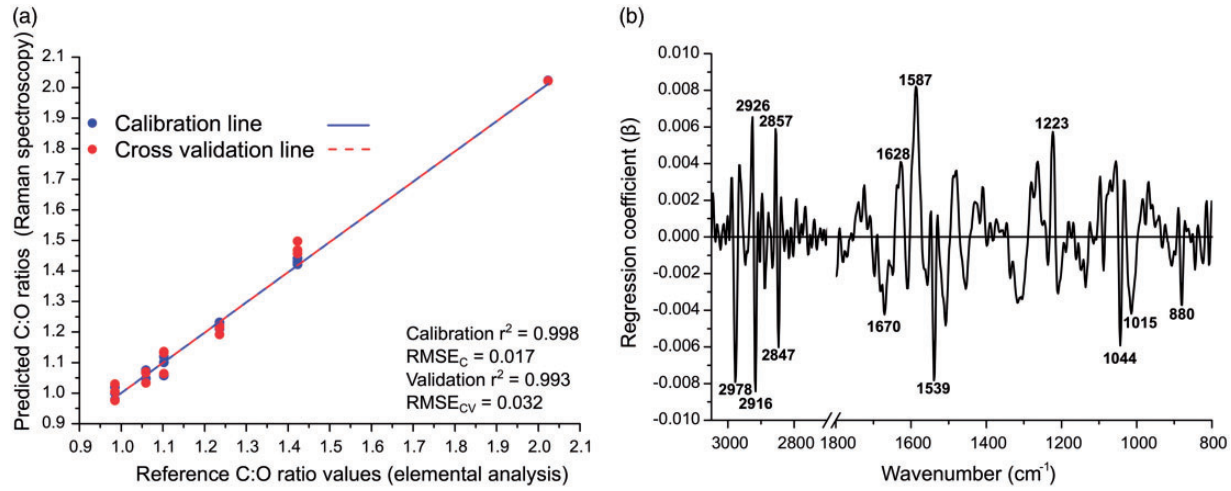

Figure 7. Summary of PLSR model relating C : O ratios of chemically reduced graphene oxide samples to IR spectral variance in the ranges of 3050–2700 and 1800–800 cm^{-1}. The (a) regression plots and (b) regression coefficient are shown.

ranges of 4000–3050 and 800–600 cm^{-1} containing no vibrational bands were removed. The spectral range of 2700–1900 cm^{-1} was removed as it contained no vibrational information, but contained a spectral artifact caused by the ATR crystal (Fig. 6c). Finally, to compensate for inter-sample variability in absolute spectral intensity, which is caused by variable contact areas between samples and the ATR crystal, spectra were normalized using a standard normal variate (SNV) transformation (Fig. 6d). These processed spectra were modeled using PLSR analysis.

A summary of the PLSR model relating ATR-IR spectral variance to C : O ratios is presented in Fig. 7. The calibration and validation plots (Fig. 7a) demonstrate a good correlation between ATR-IR spectral variance and C : O ratios by elemental analysis (validation $r^2 = 0.993$; $RMSE_{CV} = 0.032$). The regression factor loadings (Fig. 7b) were much more complex than those in the UV and Raman spectroscopy models, which made them difficult to interpret. However, it was possible to interpret some of the bands using the vibrational assignments in Table II. The more reduced CRGO samples were associated with greater peak intensities at 1628, 1587, and 1223 cm^{-1}, which are consistent with the energies of conjugated C=C stretching and aromatic ring stretches, respectively (Table II). Infrared absorption intensity at 1223 cm^{-1} was attributed to vinyl C–H bending modes (Table II). These vibrational modes were all consistent with the increased graphitic character of more highly reduced samples. The regression factor loadings associated with more oxidized CRGO samples were found at 1670, 1539, 1044, 1015, and 880 cm^{-1} (Fig. 7b). Vibrational intensity at 1670 cm^{-1} was consistent with the energy of the insulated C=C stretching. The other vibrational bands at 880, 1015, and 1044 cm^{-1} were characteristic of bending modes associated with epoxy, anhydride, and hydroxyl groups, respectively (Table II). These vibrational modes are consistent with increased GO-like character. The band at 1539 cm^{-1} could not be satisfactorily assigned.

Table II. Spectral assignment of infrared absorbance bands distinguishing graphene oxide (GO) from chemically reduced graphene oxide (CRGO).

Wavenumber (cm^{-1})	Band assignment	Associated with
880	δ (C–O–C)	GO
1015	ν (CO–O–OC)	GO
1044	ν (C–O)	GO
1223	δ (H–C=C–H)	CRGO
1539	Unknown	GO
1587	ν (C=C) aromatic	CRGO
1628	ν (C=C) conjugated	CRGO
1670	ν (C=C) insulated	GO
2700–3000	ν (C–H)	GO, CRGO

δ, in-plane bending; ν, stretching.

In summary, regression coefficient loadings for the IR PLSR model (Fig. 7b) describe how increased reduction times caused a decrease in vibrational intensity associated with epoxy, anhydride, and hydroxyl groups, and an increase in the vibrational intensity associated with conjugated double bonds and phenyl rings. These data are consistent with a gradual increase in graphitic character with increased exposure to L-AA solutions.[3,14] While a large number of previous investigations have used L-AA to reduce graphene oxide, direct comparisons of their reduction levels (oxygen concentrations) with those in this study are difficult to define. This is because the procedures used for GO/CRGO synthesis differ in reagent concentrations and ratios or reaction conditions to those used here.[3,47–49] As these factors directly affect the rate at which oxygen

groups are reduced, the resulting concentrations can differ. Further to this, the majority of published works do not quantify C/O ratios of GO/CRGOs by elemental analysis. Those that do have used surface elemental analysis such as XPS or XRD.[13,14] Also, with the exception of enzyme-related studies,[12,13,17] the reduction times reported in the literature are generally for longer durations, many simply comparing GO with reduced GO (presumably fully reduced).[3,49] While direct comparisons may be unclear, the approach to quantifying the level of reduction is still effective and to our knowledge this study is the first to assess the level of reduction in repeated L-AA reductions of GO, over a range of short and long time points.

The results from this work demonstrate that PLSR of ATR-IR spectra can be used to facilitate rapid quantitative measurements of the extent of oxidation in GO. The method is simple and allows straightforward sample presentation and nondestructive analysis. Furthermore, this approach provided insight into the functional groups that were present on the surface of GO, and with further refinement, could potentially be used to investigate which oxygen groups are most susceptible to reduction in L-AA solutions.

Conclusion

The methods described are suitable for rapid, nondestructive quantification of the amount of oxygen in GO/CRGO samples. This makes them useful tools for process control during CRGO production, especially for applications requiring precise tuning of surface hydrophobicities. Ultraviolet, Raman, and ATR-IR spectroscopy, in conjunction with PLSR and elemental analysis, could all produce models that were fit for purpose. The spectroscopic methods had different advantages relating to sample presentation, speed, and instrument availability. Attenuated total reflection IR analyses offered the most detailed insight into the reduction of GO, facilitating detection of diverse oxygen-containing groups in the GO/CRGO samples. Our findings have shown that while these methods are suitable for following the reduction of GO into CRGOs, the processing of these data through chemometric models provides a powerful approach and affords a more detailed analysis of spectral data derived from these materials. Future work could include examining which oxygen-containing functional groups reduce first, which could facilitate finer tuning of CRGO surfaces.

Conflict of Interest

The authors report that there are no conflicts of interest.

Funding

This work was supported by the Australian Research Council (LP140100722 and DP130101714) and the New Zealand Ministry for Business, Innovation, and Employment through the research program "Export Marine Products" (C11X1307).

ORCID iD

Tejaswini Rama Bangalore Ramakrishna http://orcid.org/0000-0002-9097-2844
Tim David Nalder http://orcid.org/0000-0001-8748-7429
Susan Nellette Marshall http://orcid.org/0000-0002-4155-3897

References

1. A. Furst, R.C. Berlo, S. Hooton. "Hydrazine as a Reducing Agent for Organic Compounds (Catalytic Hydrazine Reductions)". Chem. Rev. 1965. 65(1): 51–68.
2. Z.-Z. Yang, Q.-B. Zheng, H.-X. Qiu, L. Jing, et al. "A Simple Method for the Reduction of Graphene Oxide by Sodium Borohydride with $CaCl_2$ as a Catalyst". New Carbon Mater. 2015. 30(1): 41–47.
3. J. Zhang, H. Yang, G. Shen, P. Cheng, et al. "Reduction of Graphene Oxide via L-Ascorbic Acid". Chem. Comm. 2010. 46(7): 1112–1114.
4. M.D. Stoller, S. Park, Y. Zhu, J. An, et al. "Graphene-Based Ultracapacitors". Nano Lett. 2008. 8(10): 3498–3502.
5. F. Li, X. Jiang, J. Zhao, S. Zhang. "Graphene Oxide: A Promising Nanomaterial for Energy and Environmental Applications". Nano Energy. 2015. 16: 488–515.
6. R. Ghosh, A. Midya, S. Santra, S.K. Ray, et al. "Chemically Reduced Graphene Oxide for Ammonia Detection at Room Temperature". ACS Appl. Mater. Inter. 2013. 5(15): 7599–7603.
7. M. Zhou, Y. Zhai, S. Dong. "Electrochemical Sensing and Biosensing Platform Based on Chemically Reduced Graphene Oxide". Anal. Chem. 2009. 81(14): 5603–5613.
8. N. Kong, M. Vaka, N.D. Nam, C.J. Barrow, et al. "Controllable Graphene Oxide Mediated Efficient Electron Transfer Pathways across Self-Assembly Monolayers: A New Class of Graphene Based Electrodes". Electrochim. Acta. 2016. 210(Suppl.C): 539–547.
9. D. Joung, A. Chunder, L. Zhai, S.I. Khondaker. "High Yield Fabrication of Chemically Reduced Graphene Oxide Field Effect Transistors by Dielectrophoresis". Nanotechnology. 2010. 21(16): 165202.
10. V.C. Tung, M.J. Allen, Y. Yang, R.B. Kaner. "High-Throughput Solution Processing of Large-Scale Graphene". Nat. Nanotechnol. 2009. 4(1): 25–29.
11. J. Wang, E.C. Salihi, L. Šiller. "Green Reduction of Graphene Oxide Using Alanine". Mater. Sci. Eng. C. 2017. 72: 1–6.
12. Y. Zhang, J. Zhang, X. Huang, X. Zhou, et al. "Assembly of Graphene Oxide–Enzyme Conjugates Through Hydrophobic Interaction". Small. 2012. 8(1): 154–159.
13. M. Mathesh, B. Luan, T.O. Akanbi, J.K. Weber, et al. "Opening Lids: Modulation of Lipase Immobilization by Graphene Oxides". ACS Catal. 2016. 6(7): 4760–4768.
14. Z. Liu, J. Liu, D. Li, P.S. Francis, et al. "Probing the Tunable Surface Chemistry of Graphene Oxide". Chem. Comm. 2015. 51(54): 10969–10972.
15. J. Liu, H. Ma, H. Zhu, Z. Liu, et al. "Quantifying the Tunable Conjugated Area of Graphene Oxide by Using Pyrene as a Fluorescent Probe". Chem. Eur. J. 2016. 22(52): 18881–18886.
16. M. Mathesh, J. Liu, C.J. Barrow, W. Yang. "Graphene-Oxide-Based Enzyme Nanoarchitectonics for Substrate Channeling". Chem. Eur. J. 2017. 23(2): 304–311.
17. F. Zhao, H. Li, Y. Jiang, X. Wang, et al. "Co-Immobilization of Multi-Enzyme on Control-Reduced Graphene Oxide by Non-Covalent Bonds: An Artificial Biocatalytic System for the One-Pot Production of Gluconic Acid from Starch". Green Chem. 2014. 16(5): 2558–2565.
18. I.K. Moon, J. Lee, R.S. Ruoff, H. Lee. "Reduced Graphene Oxide by Chemical Graphitization". Nat. Commun. 2010. 1: 73.
19. W. Chen, L. Yan, P. Bangal. "Chemical Reduction of Graphene Oxide to Graphene by Sulfur-Containing Compounds". J. Phys. Chem. C. 2010. 114(47): 19885–19890.

20. C. Botas, P. Álvarez, C. Blanco, M.D. Gutiérrez, et al. "Tailored Graphene Materials by Chemical Reduction of Graphene Oxides of Different Atomic Structure". RSC Adv. 2012. 2(25): 9643–9650.
21. S. Bae, H. Kim, Y. Lee, X. Xu, et al. "Roll-to-Roll Production of 30-inch Graphene Films for Transparent Electrodes". Nat. Nanotechnol. 2010. 5: 574.
22. D. Yang, A. Velamakanni, G. Bozoklu, S. Park, et al. "Chemical Analysis of Graphene Oxide Films after Heat and Chemical Treatments by X-ray Photoelectron and Micro-Raman Spectroscopy". Carbon. 2009. 47(1): 145–152.
23. S. Stankovich, D.A. Dikin, R.D. Piner, K.A. Kohlhaas, et al. "Synthesis of Graphene-Based Nanosheets via Chemical Reduction of Exfoliated Graphite Oxide". Carbon. 2007. 45(7): 1558–1565.
24. A. Kozbial, Z. Li, C. Conaway, R. McGinley, et al. "Study on the Surface Energy of Graphene by Contact Angle Measurements". Langmuir. 2014. 30(28): 8598–8606.
25. J.-S. Lee, J.-C. Yoon, J.-H. Jang. "A Route Towards Superhydrophobic Graphene Surfaces: Surface-Treated Reduced Graphene Oxide Spheres". J. Mater. Chem. A. 2013. 1(25): 7312–7315.
26. J. Rafiee, X. Mi, H. Gullapalli, A.V. Thomas, et al. "Wetting Transparency of Graphene". Nat. Mater. 2012. 11: 217.
27. G. Wang, J. Yang, J. Park, X. Gou, et al. "Facile Synthesis and Characterization of Graphene Nanosheets". J. Phys. Chem. C. 2008. 112(22): 8192–8195.
28. D.A. Dikin, S. Stankovich, E.J. Zimney, R.D. Piner, et al. "Preparation and Characterization of Graphene Oxide Paper". Nature. 2007. 448: 457.
29. S. Park, J. An, J.R. Potts, A. Velamakanni, et al. "Hydrazine-Reduction of Graphite- and Graphene Oxide". Carbon. 2011. 49(9): 3019–3023.
30. D.C. Marcano, D.V. Kosynkin, J.M. Berlin, A. Sinitskii, et al. "Improved Synthesis of Graphene Oxide". ACS Nano. 2010. 4(8): 4806–4814.
31. S. Yang, X. Feng, S. Ivanovici, K. Müllen. "Fabrication of Graphene-Encapsulated Oxide Nanoparticles: Towards High-Performance Anode Materials for Lithium Storage". Angew. Chem. Int. Ed. 2010. 49(45): 8408–8411.
32. R. Gao, N. Hu, Z. Yang, Q. Zhu, et al. "Paper-Like Graphene-Ag Composite Films with Enhanced Mechanical and Electrical Properties". Nanoscale Res. Lett. 2013. 8(1): 32.
33. I. Horcas, R. Fernández, J. Gomez-Rodriguez, J. Colchero, et al. "WSXM: A Software for Scanning Probe Microscopy and a Tool for Nanotechnology". Rev. Sci. Instrum. 2007. 78(1): 013705.
34. C. Gómez-Navarro, R.T. Weitz, A.M. Bittner, M. Scolari, et al. "Electronic Transport Properties of Individual Chemically Reduced Graphene Oxide Sheets". Nano Lett. 2007. 7(11): 3499–3503.
35. G. Eda, G. Fanchini, M. Chhowalla. "Large-Area Ultrathin Films of Reduced Graphene Oxide as a Transparent and Flexible Electronic Material". Nat. Nanotechnol. 2008. 3(5): 270–274.
36. H. He, T. Riedl, A. Lerf, J. Klinowski. "Solid-State NMR Studies of the Structure of Graphite Oxide". J. Phys. Chem. 1996. 100(51): 19954–19958.
37. A. Lerf, H. He, T. Riedl, M. Forster, et al. "13C and 1H MAS NMR Studies of Graphite Oxide and Its Chemically Modified Derivatives". Solid State Ionics. 1997. 101: 857–862.
38. L.B. Casabianca, M.A. Shaibat, W.W. Cai, S. Park, et al. "NMR-Based Structural Modeling of Graphite Oxide Using Multidimensional 13C Solid-State NMR and Ab Initio Chemical Shift Calculations". J. Am. Chem. Soc. 2010. 132(16): 5672–5676.
39. J.I. Paredes, S. Villar-Rodil, A. Martínez-Alonso, J.M.D. Tascón. "Graphene Oxide Dispersions in Organic Solvents". Langmuir. 2008. 24(19): 10560–10564.
40. S. Stankovich, R.D. Piner, X. Chen, N. Wu, et al. "Stable Aqueous Dispersions of Graphitic Nanoplatelets Via the Reduction of Exfoliated Graphite Oxide in the Presence of Poly(Sodium 4-Styrenesulfonate)". J. Mater. Chem. 2006. 16(2): 155–158.
41. D. Li, M.B. Müller, S. Gilje, R.B. Kaner, et al. "Processable Aqueous Dispersions of Graphene Nanosheets". Nat. Nanotechnol. 2008. 3(2): 101–105.
42. Y. Si, E.T. Samulski. "Synthesis of Water Soluble Graphene". Nano Lett. 2008. 8(6): 1679–1682.
43. S. Eigler, A.M. Dimiev. "Characterization Techniques". In: S. Eigler, A.M. Dimiev, editors. Graphene Oxide: Fundamentals and Applications. Chichester, UK: John Wiley and Sons, Ltd, 2016, pp.85–120.
44. L. Shahriary, A.A. Athawale. "Graphene Oxide Synthesized by Using Modified Hummers Approach". Int. J. Renew. Energy Environ. Eng. 2014. 2(01): 58–63.
45. Q. Lai, S. Zhu, X. Luo, M. Zou, et al. "Ultraviolet–Visible Spectroscopy of Graphene Oxides". AIP Adv. 2012. 2(3): 032146.
46. L. Bokobza, J.-L. Bruneel, M. Couzi. "Raman Spectroscopy as a Tool for the Analysis of Carbon-Based Materials(Highly Oriented Pyrolitic Graphite, Multilayer Graphene and Multiwall Carbon Nanotubes) and of Some of Their Elastomeric Composites". Vib. Spectrosc. 2014. 74: 57–63.
47. M.J. Fernández-Merino, L. Guardia, J.I. Paredes, S. Villar-Rodil, et al. "Vitamin C Is an Ideal Substitute for Hydrazine in the Reduction of Graphene Oxide Suspensions". J. Phys. Chem. C. 2010. 114(14): 6426–6432.
48. K. De Silva, H.-H. Huang, R. Joshi, M. Yoshimura. "Chemical Reduction of Graphene Oxide Using Green Reductants". Carbon. 2017. 119: 190–199.
49. C. Xu, X. Shi, A. Ji, L. Shi, et al. "Fabrication and Characteristics of Reduced Graphene Oxide Produced with Different Green Reductants". PLoS One. 2015. 10(12): e0144842.